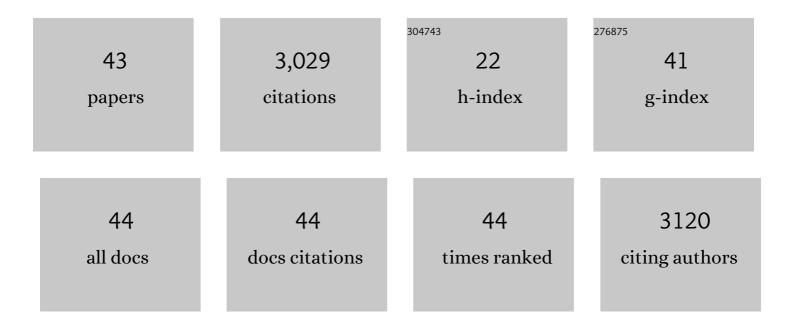
Dominic Papineau

List of Publications by Year in descending order

Source: https://exaly.com/author-pdf/7211460/publications.pdf Version: 2024-02-01



| # | Article | IF | CITATIONS |
|----|---|------|-----------|
| 1 | Biosignatures Associated with Organic Matter in Late Paleoproterozoic Stromatolitic Dolomite and Implications for Martian Carbonates. Astrobiology, 2022, 22, 49-74. | 3.0 | 7 |
| 2 | Cyanobacterial spheroids and other biosignatures from microdigitate stromatolites of Mesoproterozoic Wumishan Formation in Jixian, North China. Precambrian Research, 2022, 368, 106496. | 2.7 | 7 |
| 3 | Extensive primary production promoted the recovery of the Ediacaran Shuram excursion. Nature Communications, 2022, 13, 148. | 12.8 | 14 |
| 4 | Metabolically diverse primordial microbial communities in Earth's oldest seafloor-hydrothermal jasper. Science Advances, 2022, 8, eabm2296. | 10.3 | 24 |
| 5 | Characteristics of the carbon cycle in late Mesoproterozoic: Evidence from carbon isotope composition of paired carbonate and organic matter of the Shennongjia Group in South China. Precambrian Research, 2022, 377, 106726. | 2.7 | 5 |
| 6 | Organic diagenesis in stromatolitic dolomite and chert from the late Palaeoproterozoic McLeary Formation. Precambrian Research, 2021, 354, 106052. | 2.7 | 6 |
| 7 | Chemically Oscillating Reactions during the Diagenetic Formation of Ediacaran Siliceous and Carbonate Botryoids. Minerals (Basel, Switzerland), 2021, 11, 1060. | 2.0 | 9 |
| 8 | Transformation of protodolomite to dolomite proceeds under dry-heating conditions. Earth and Planetary Science Letters, 2021, 576, 117249. | 4.4 | 15 |
| 9 | Precipitation of protodolomite facilitated by sulfate-reducing bacteria: The role of capsule extracellular polymeric substances. Chemical Geology, 2020, 533, 119415. | 3.3 | 31 |
| 10 | Dynamic carbon and sulfur cycling in the aftermath of the Lomagundi-Jatuli Event: Evidence from the Paleoproterozoic Hutuo Supergroup, North China Craton. Precambrian Research, 2020, 337, 105549. | 2.7 | 6 |
| 11 | Abiotic and biotic processes that drive carboxylation and decarboxylation reactions. American Mineralogist, 2020, 105, 609-615. | 1.9 | 13 |
| 12 | Chemically oscillating reactions in the formation of botryoidal malachite. American Mineralogist, 2020, 105, 447-454. | 1.9 | 14 |
| 13 | Apatite-glaucony association in the Ediacaran Doushantuo Formation, South China and implications for marine redox conditions. Precambrian Research, 2020, 347, 105842. | 2.7 | 13 |
| 14 | Catalytic effect of microbially-derived carboxylic acids on the precipitation of Mg-calcite and disordered dolomite: Implications for sedimentary dolomite formation. Journal of Asian Earth Sciences, 2020, 193, 104301. | 2.3 | 15 |
| 15 | The catalytic role of planktonic aerobic heterotrophic bacteria in protodolomite formation: Results from Lake Jibuhulangtu Nuur, Inner Mongolia, China. Geochimica Et Cosmochimica Acta, 2019, 263, 31-49. | 3.9 | 35 |
| 16 | Deciphering Biosignatures in Planetary Contexts. Astrobiology, 2019, 19, 1075-1102. | 3.0 | 66 |
| 17 | Minimal biomass deposition in banded iron formations inferred from organic matter and clay relationships. Nature Communications, 2019, 10, 5022. | 12.8 | 11 |
| 18 | Fossil biomass preserved as graphitic carbon in a late Paleoproterozoic banded iron formation metamorphosed at more than 550°C. Journal of the Geological Society, 2019, 176, 651-668. | 2.1 | 5 |

DOMINIC PAPINEAU

| # | Article | IF | CITATIONS |
|----|---|------|-----------|
| 19 | Widespread occurrences of variably crystalline 13C-depleted graphitic carbon in banded iron formations. Earth and Planetary Science Letters, 2019, 512, 163-174. | 4.4 | 28 |
| 20 | Experimental evidence for abiotic formation of low-temperature proto-dolomite facilitated by clay minerals. Geochimica Et Cosmochimica Acta, 2019, 247, 83-95. | 3.9 | 81 |
| 21 | An integrated chemostratigraphic (δ13C-δ18O-87Sr/86Sr-δ15N) study of the Doushantuo Formation in western Hubei Province, South China. Precambrian Research, 2019, 320, 232-252. | 2.7 | 22 |
| 22 | Organic remains in late Palaeoproterozoic granular iron formations and implications for the origin of granules. Precambrian Research, 2018, 310, 133-152. | 2.7 | 20 |
| 23 | Evidence for early life in Earth's oldest hydrothermal vent precipitates. Nature, 2017, 543, 60-64. | 27.8 | 522 |
| 24 | Chemically-oscillating reactions during the diagenetic oxidation of organic matter and in the formation of granules in late Palaeoproterozoic chert from Lake Superior. Chemical Geology, 2017, 470, 33-54. | 3.3 | 27 |
| 25 | The termination and aftermath of the Lomagundi-Jatuli carbon isotope excursions in the Paleoproterozoic Hutuo Group, North China. Journal of Earth Science (Wuhan, China), 2016, 27, 297-316. | 3.2 | 14 |
| 26 | New observations of Ambient Inclusion Trails (AITs) and pyrite framboids in the Ediacaran Doushantuo Formation, South China. Palaeogeography, Palaeoclimatology, Palaeoecology, 2016, 461, 374-388. | 2.3 | 8 |
| 27 | High-precision analysis of multiple sulfur isotopes using NanoSIMS. Chemical Geology, 2016, 420, 148-161. | 3.3 | 35 |
| 28 | Terminal Proterozoic cyanobacterial blooms and phosphogenesis documented by the Doushantuo granular phosphorites II: Microbial diversity and C isotopes. Precambrian Research, 2014, 251, 62-79. | 2.7 | 39 |
| 29 | Terminal Proterozoic cyanobacterial blooms and phosphogenesis documented by the Doushantuo granular phosphorites I: In situ micro-analysis of textures and composition. Precambrian Research, 2013, 235, 20-35. | 2.7 | 61 |
| 30 | Biological carbon precursor to diagenetic siderite with spherical structures in iron formations. Nature Communications, 2013, 4, 1741. | 12.8 | 85 |
| 31 | High phosphate availability as a possible cause for massive cyanobacterial production of oxygen in the Paleoproterozoic atmosphere. Earth and Planetary Science Letters, 2013, 362, 225-236. | 4.4 | 50 |
| 32 | 7.7 The Earliest Phosphorites: Radical Change in the Phosphorus Cycle During the Palaeoproterozoic. Frontiers in Earth Sciences, 2013, , 1275-1296. | 0.1 | 2 |
| 33 | A Chronostratigraphic Division of the Precambrian. , 2012, , 299-392. | | 69 |
| 34 | Carbon isotope geochemistry and geochronological constraints of the Neoproterozoic Sirohi Group from northwest India. Precambrian Research, 2012, 220-221, 80-90. | 2.7 | 41 |
| 35 | Global Biogeochemical Changes at Both Ends of the Proterozoic: Insights from Phosphorites. Astrobiology, 2010, 10, 165-181. | 3.0 | 150 |
| 36 | Ancient graphite in the Eoarchean quartz–pyroxene rocks from Akilia in southern West Greenland I: Petrographic and spectroscopic characterization. Geochimica Et Cosmochimica Acta, 2010, 74, 5862-5883. | 3.9 | 55 |

DOMINIC PAPINEAU

| # | Article | IF | CITATIONS |
|----|--|------|-----------|
| 37 | Ancient graphite in the Eoarchean quartz-pyroxene rocks from Akilia in southern West Greenland II: Isotopic and chemical compositions and comparison with Paleoproterozoic banded iron formations. Geochimica Et Cosmochimica Acta, 2010, 74, 5884-5905. | 3.9 | 47 |
| 38 | Oceanic nickel depletion and a methanogen famine before the Great Oxidation Event. Nature, 2009, 458, 750-753. | 27.8 | 397 |
| 39 | High primary productivity and nitrogen cycling after the Paleoproterozoic phosphogenic event in the Aravalli Supergroup, India. Precambrian Research, 2009, 171, 37-56. | 2.7 | 76 |
| 40 | Mineral evolution. American Mineralogist, 2008, 93, 1693-1720. | 1.9 | 569 |
| 41 | Session 15. The Evolution of the Biogeochemical Cycling of Phosphorus and Other Bioessential Elements. Astrobiology, 2008, 8, 356-361. | 3.0 | 0 |
| 42 | Multiple sulfur isotopes from Paleoproterozoic Huronian interglacial sediments and the rise of atmospheric oxygen. Earth and Planetary Science Letters, 2007, 255, 188-212. | 4.4 | 127 |
| 43 | Composition and Structure of Microbial Communities from Stromatolites of Hamelin Pool in Shark Bay, Western Australia. Applied and Environmental Microbiology, 2005, 71, 4822-4832. | 3.1 | 203 |